Supplementary Materials

Graphene-based flexible magnetic tactile sensor with vertically periodic magnetization for enhanced spatial resolution

Xuejiao Li[1,#], Wenwei Gao[1,#], Biyan Wang[1], Wenlong Jiao[2], Hong Su[3], Wenbiao Zhou[1], Huikai Xie[1,2], Yajing Shen[4,*], Xiaoyi Wang[1,2,*]

[1]The School of Integrated Circuits and Electronics, Beijing Institute of Technology, Beijing 100081, China.

[2]BIT Chongqing Institute of Microelectronics and Microsystems, Chongqing 400030, China.

[3]Scientific Research Department, Peking University School and Hospital of Stomatology, Beijing 100081, China.

[4]Department of Electronic and Computer Engineering, The Hong Kong University of Science and Technology, Hong Kong 999077, China.

[#]These authors contributed equally to this work.

[*]**Correspondence to:** Prof. Yajing Shen, Department of Electronic and Computer Engineering, The Hong Kong University of Science and Technology, Hong Kong 999077, China. E-mail: eeyajing@ust.hk; Prof. Xiaoyi Wang, The School of Integrated Circuits and Electronics, Beijing Institute of Technology, Beijing 100081, China. E-mail: xiaoyiwang@bit.edu.cn

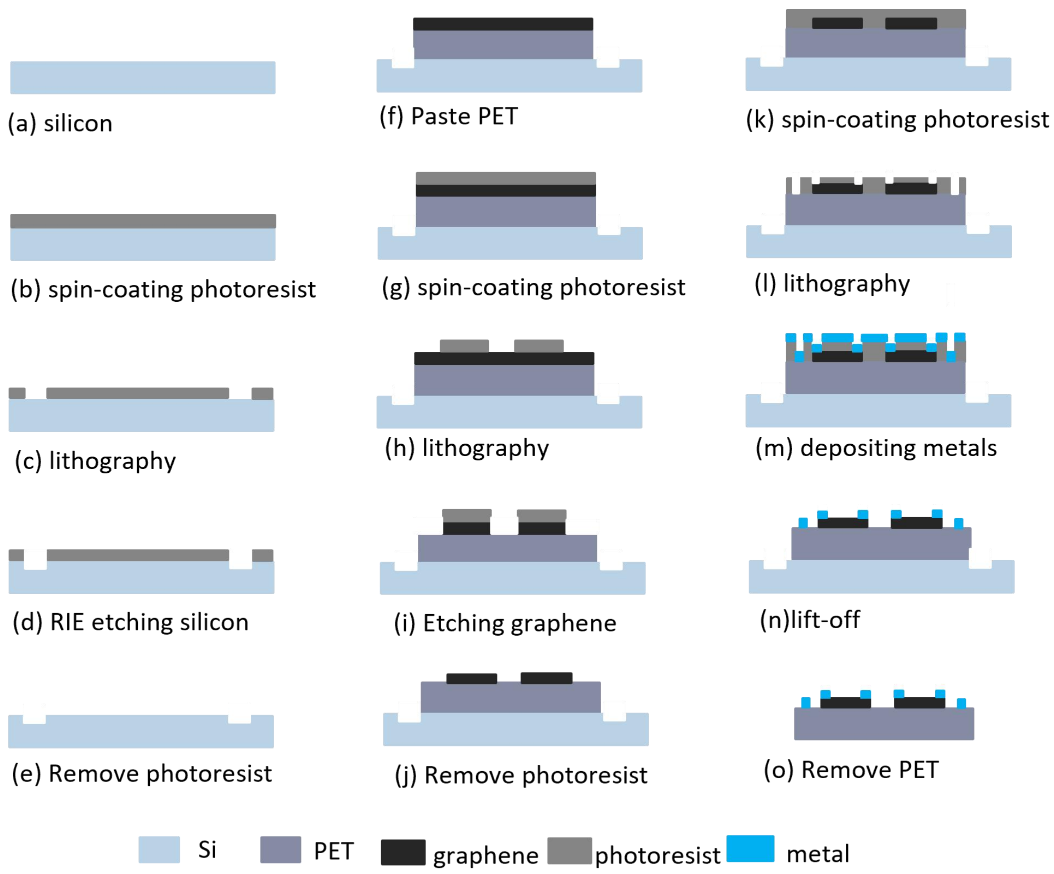

Supplementary Figure 1. Process Flow of graphene-based hall sensor.

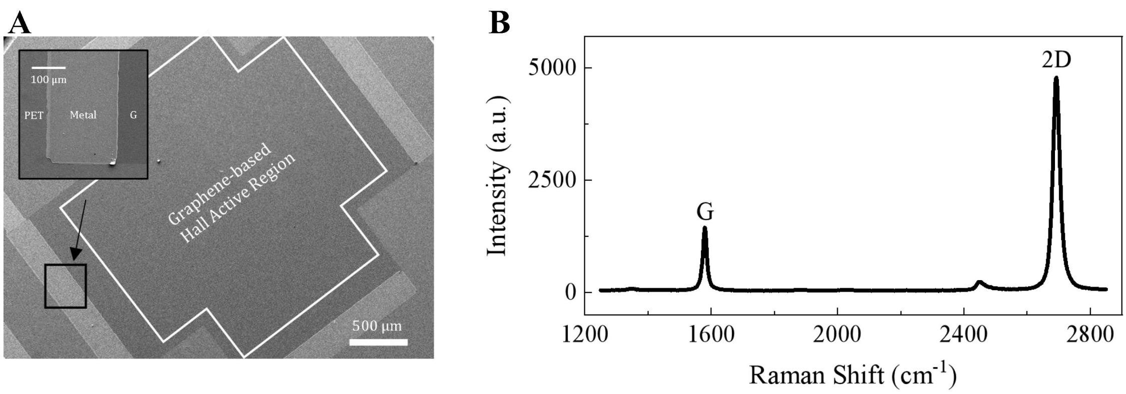

Supplementary Figure 2. (A) SEM image of the graphene-based Hall sensor; (B) Raman characterization results of graphene.

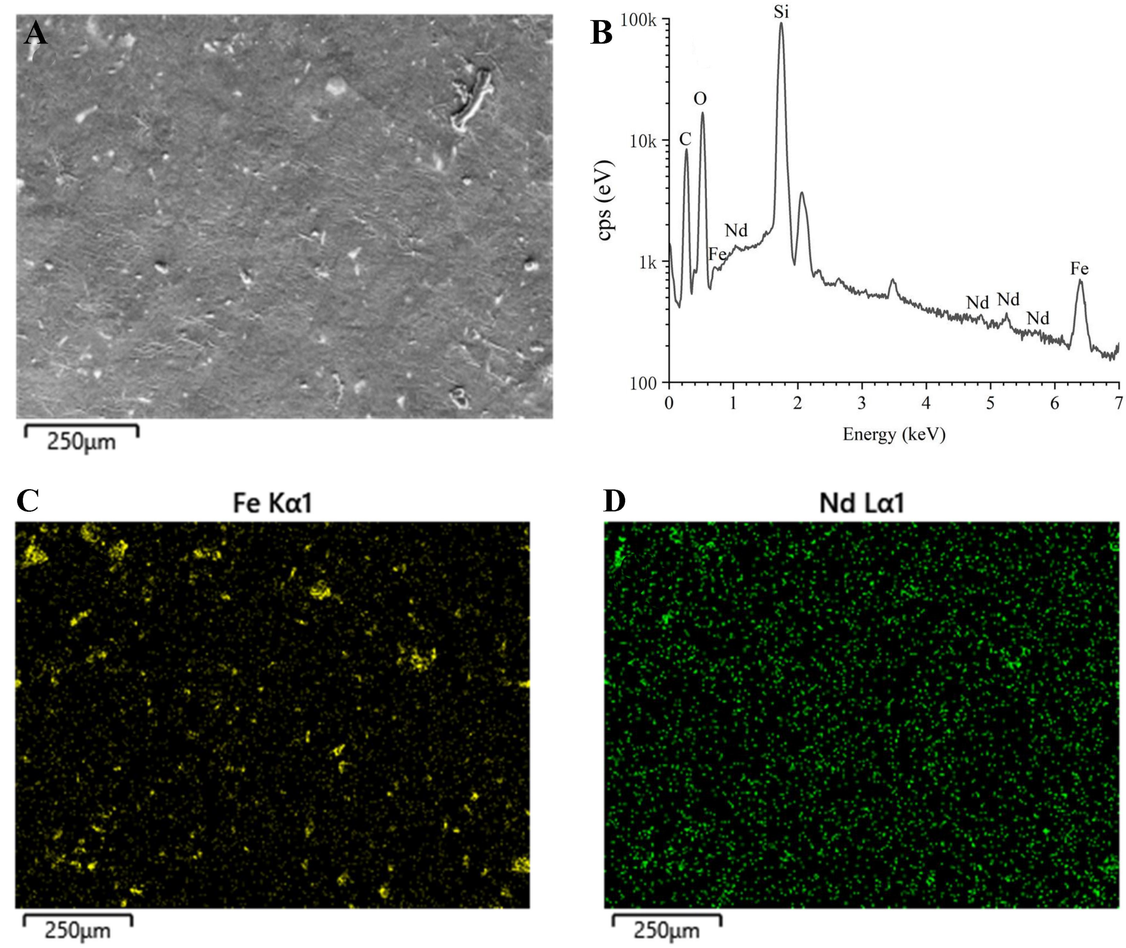

Supplementary Figure 3. EDS analysis results of the magnetic film: (A) SEM image; (B) EDS spectrum; (C and D) show the distribution of Fe, and Nd, respectively.

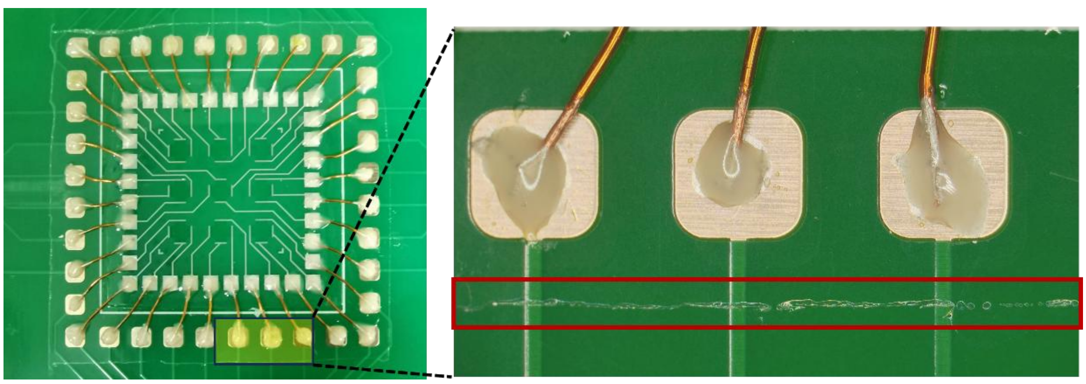

Supplementary Figure 4. Parylene-C deposition results.

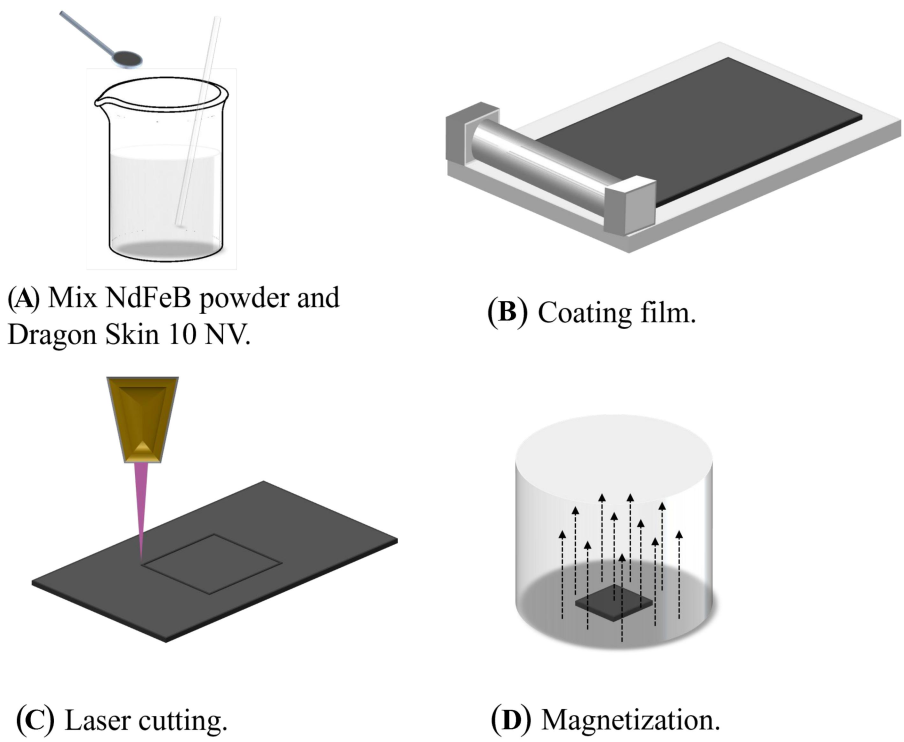

Supplementary Figure 5. Fabrication of magnetic films.

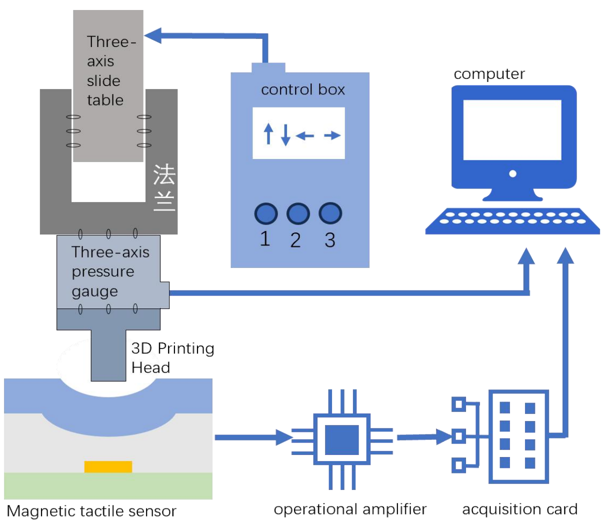

Supplementary Figure 6. Test system.

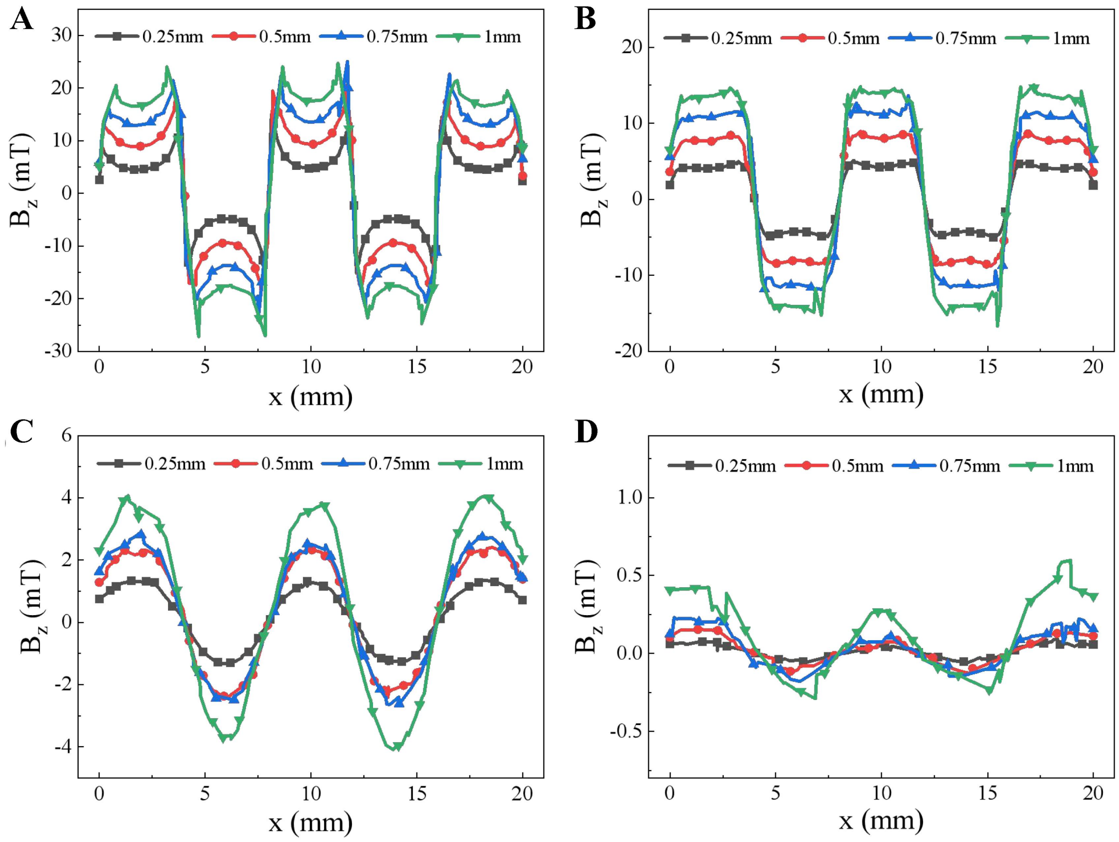

Supplementary Figure 7. Comparison of z-axis magnetic field simulations at different heights for different thicknesses of magnetic films. (A) h1 = 0.1 mm. (B) h2 = 0.5 mm. (C) h3 = 2 mm. (D) h4 = 5 mm.

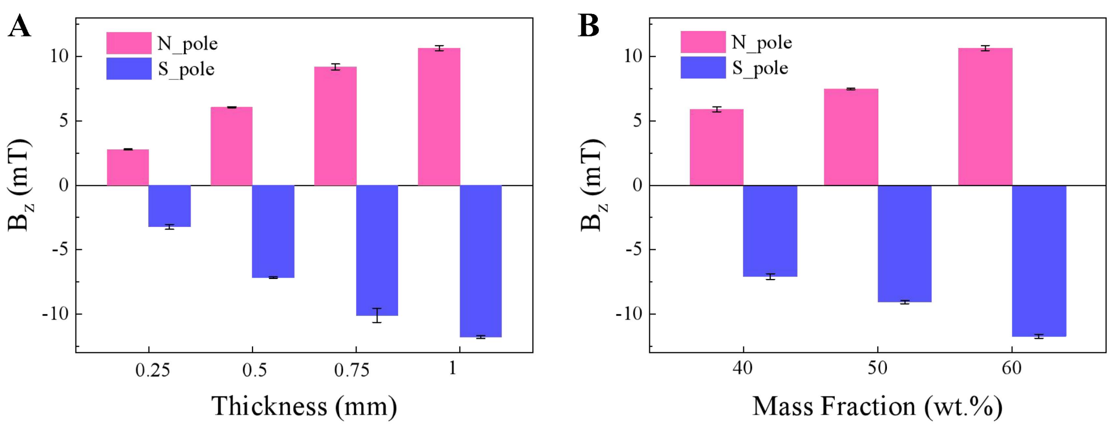

Supplementary Figure 8. Test results of z-axis magnetic field for (A) different thicknesses and (B) different mass fractions of magnetic films.

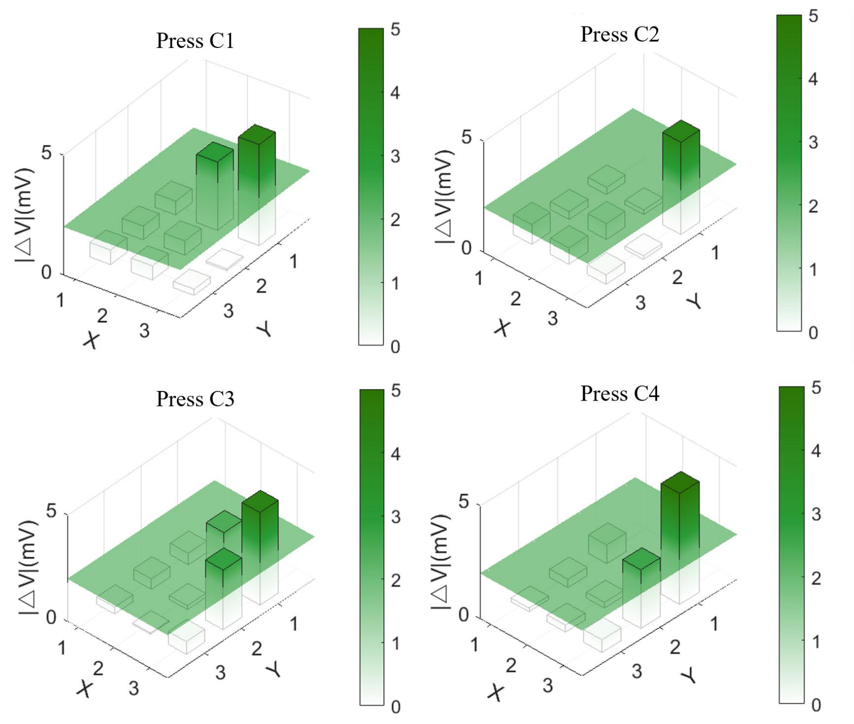

Supplementary Figure 9. Output comparison of pressing C1-C4.

Supplementary Table 1. Judgmental conditions for press C1-C4

Condition	Result
$\lvert\Delta V_{H3}\rvert>\lvert\Delta V_{Hi,i=1,2,4-9}\rvert$, $\lvert\Delta V_{H2}\rvert>V_{h_3}$, $\lvert\Delta V_{Hj,j=1,4-9}\rvert<V_{h_3}$	C1
$\lvert\Delta V_{H3}\rvert>\lvert\Delta V_{Hi,i=1,2,4-9}\rvert$, $\lvert\Delta V_{Hj,j=1,2,4-9}\rvert<V_{h_3}$	C2
$\lvert\Delta V_{H3}\rvert>\lvert\Delta V_{Hi,i=1,2,4-9}\rvert$, $\lvert\Delta V_{H2}\rvert>V_{h_3}$, $\lvert\Delta V_{H6}\rvert>V_{h_3}$, $\lvert\Delta V_{Hj,j=1,4,5,7-9}\rvert<V_{h_3}$	C3
$\lvert\Delta V_{H3}\rvert>\lvert\Delta V_{Hi,i=1,2,4-9}\rvert$, $\lvert\Delta V_{H6}\rvert>V_{h_3}$, $\lvert\Delta V_{Hj,j=1,2,4,5,7-9}\rvert<V_{h_3}$	C4

Supplementary Table 2. Judgmental conditions for press C1-C4

Condition	Result
$\lvert\Delta V_{H7}\rvert>\lvert\Delta V_{Hi,i=1-6,8-9}\rvert$, $\lvert\Delta V_{H4}\rvert>V_{h_7}$, $\lvert\Delta V_{Hj,j=1-3,5,6,8,9}\rvert<V_{h_7}$	G1
$\lvert\Delta V_{H7}\rvert>\lvert\Delta V_{Hi,i=1-6,8-9}\rvert$, $\lvert\Delta V_{H4}\rvert>V_{h_7}$, $\lvert\Delta V_{H8}\rvert>V_{h_7}$, $\lvert\Delta V_{Hj,j=1-3,5,6,9}\rvert<V_{h_7}$	G2
$\lvert\Delta V_{H7}\rvert>\lvert\Delta V_{Hi,i=1-6,8-9}\rvert$, $\lvert\Delta V_{Hj,j=1-6,8-9}\rvert<V_{h_7}$	G3
$\lvert\Delta V_{H7}\rvert>\lvert\Delta V_{Hi,i=1-6,8-9}\rvert$, $\lvert\Delta V_{H8}\rvert>V_{h_7}$, $\lvert\Delta V_{Hj,j=1-6,9}\rvert<V_{h_7}$	G4

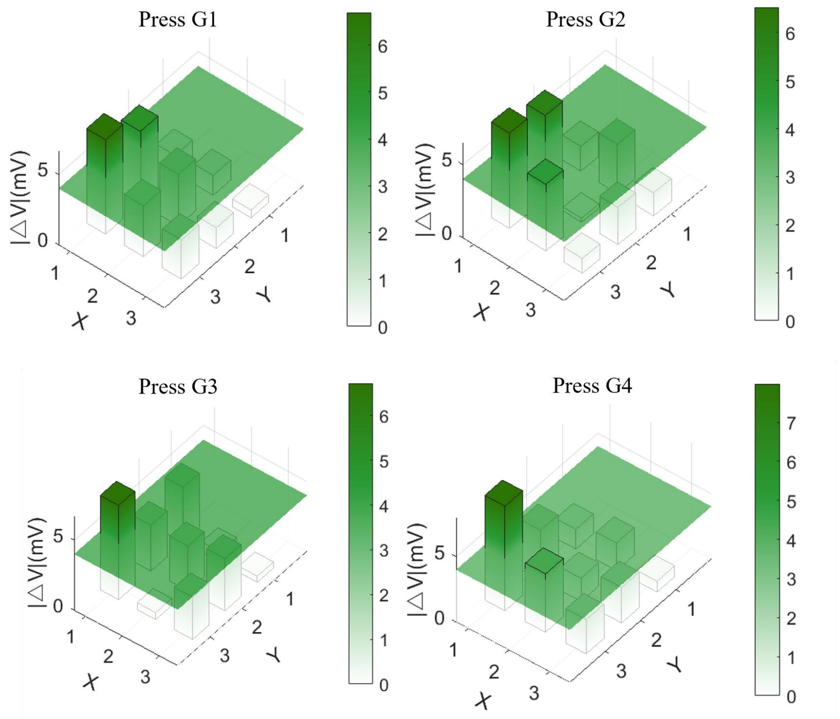

Supplementary Figure 10. Output comparison of pressing G1-G4.

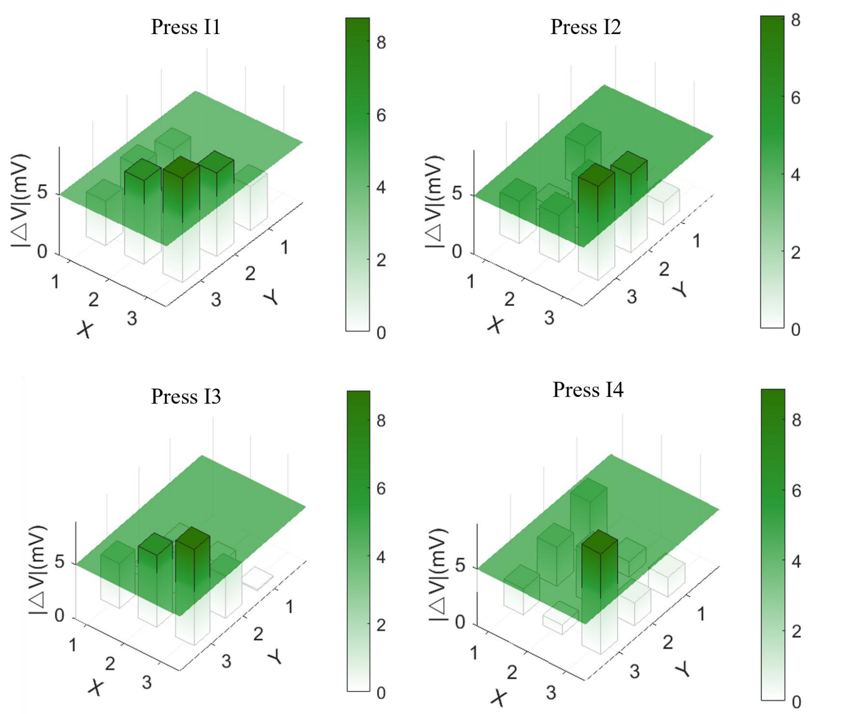

Supplementary Figure 11. Output comparison of pressing I1-I4.

Supplementary Table 3. Judgmental conditions for press I1-I4

Condition	Result
$\lvert\Delta V_{H9}\rvert > \lvert\Delta V_{Hi,i=1-8}\rvert$, $\lvert\Delta V_{H6}\rvert > V_{h_9}$, $\lvert\Delta V_{H8}\rvert > V_{h_9}$, $\lvert\Delta V_{Hj,j=1-5,7}\rvert < V_{h_9}$	I1
$\lvert\Delta V_{H9}\rvert > \lvert\Delta V_{Hi,i=1-8}\rvert$, $\lvert\Delta V_{H6}\rvert > V_{h_9}$, $\lvert\Delta V_{Hj,j=1-5,7,8}\rvert < V_{h_9}$	I2
$\lvert\Delta V_{H9}\rvert > \lvert\Delta V_{Hi,i=1-8}\rvert$, $\lvert\Delta V_{H8}\rvert > V_{h_9}$, $\lvert\Delta V_{Hj,j=1-7}\rvert < V_{h_9}$	I3
$\lvert\Delta V_{H9}\rvert > \lvert\Delta V_{Hi,i=1-8}\rvert$, $\lvert\Delta V_{Hj,j=1-8}\rvert < V_{h_9}$	I4

Supplementary Table 4. Judgmental conditions for press D1-D4

Condition	Result
$\lvert\Delta V_{H4}\rvert > \lvert\Delta V_{Hi,i=1-3,5-9}\rvert$, $\lvert\Delta V_{H1}\rvert > V_{h_4}$, $\lvert\Delta V_{Hj,j=2,3,5-9}\rvert < V_{h_4}$	D1
$\lvert\Delta V_{H4}\rvert > \lvert\Delta V_{Hi,i=1-3,5-9}\rvert$, $\lvert\Delta V_{H1}\rvert > V_{h_4}$, $\lvert\Delta V_{H5}\rvert > V_{h_4}$, $\lvert\Delta V_{Hj,j=2,3,6-9}\rvert < V_{h_4}$	D2
$\lvert\Delta V_{H4}\rvert > \lvert\Delta V_{Hi,i=1-3,5-9}\rvert$, $\lvert\Delta V_{H7}\rvert > V_{h_4}$, $\lvert\Delta V_{Hj,j=1-3,5,6,8,9}\rvert < V_{h_4}$	D3
$\lvert\Delta V_{H4}\rvert > \lvert\Delta V_{Hi,i=1-3,5-9}\rvert$, $\lvert\Delta V_{H5}\rvert > V_{h_4}$, $\lvert\Delta V_{H7}\rvert > V_{h_4}$, $\lvert\Delta V_{Hj,j=1-3,6,8,9}\rvert < V_{h_4}$	D4

Supplementary Table 5. Judgmental conditions for press F1-F4

Condition	Result
$\lvert\Delta V_{H6}\rvert > \lvert\Delta V_{Hi,i=1-5,7-9}\rvert$, $\lvert\Delta V_{H3}\rvert > V_{h_6}$, $\lvert\Delta V_{H5}\rvert > V_{h_6}$, $\lvert\Delta V_{Hj,j=1,2,4,7-9}\rvert < V_{h_6}$	F1
$\lvert\Delta V_{H6}\rvert > \lvert\Delta V_{Hi,i=1-5,7-9}\rvert$, $\lvert\Delta V_{H3}\rvert > V_{h_6}$, $\lvert\Delta V_{Hj,j=1,2,4,5,7-9}\rvert < V_{h_6}$	F2
$\lvert\Delta V_{H6}\rvert > \lvert\Delta V_{Hi,i=1-5,7-9}\rvert$, $\lvert\Delta V_{H5}\rvert > V_{h_6}$, $\lvert\Delta V_{H9}\rvert > V_{h_6}$, $\lvert\Delta V_{Hj,j=1-4,7,8}\rvert < V_{h_6}$	F3
$\lvert\Delta V_{H6}\rvert > \lvert\Delta V_{Hi,i=1-5,7-9}\rvert$, $\lvert\Delta V_{H9}\rvert > V_{h_6}$, $\lvert\Delta V_{Hj,j=1-5,7,8}\rvert < V_{h_6}$	F4

Supplementary Table 6. Judgmental conditions for press H1-H4

Condition	Result
$\lvert\Delta V_{H8}\rvert > \lvert\Delta V_{Hi,i=1-7,9}\rvert$, $\lvert\Delta V_{H5}\rvert > V_{h_8}$, $\lvert\Delta V_{H7}\rvert > V_{h_8}$, $\lvert\Delta V_{Hj,j=1-4,6,9}\rvert < V_{h_8}$	H1
$\lvert\Delta V_{H8}\rvert > \lvert\Delta V_{Hi,i=1-7,9}\rvert$, $\lvert\Delta V_{H5}\rvert > V_{h_8}$, $\lvert\Delta V_{H9}\rvert > V_{h_8}$, $\lvert\Delta V_{Hj,j=1-4,6,7}\rvert < V_{h_8}$	H2
$\lvert\Delta V_{H8}\rvert > \lvert\Delta V_{Hi,i=1-7,9}\rvert$, $\lvert\Delta V_{H7}\rvert > V_{h_8}$, $\lvert\Delta V_{Hj,j=1-6,9}\rvert < V_{h_8}$	H3
$\lvert\Delta V_{H8}\rvert > \lvert\Delta V_{Hi,i=1-7,9}\rvert$, $\lvert\Delta V_{H9}\rvert > V_{h_8}$, $\lvert\Delta V_{Hj,j=1-7}\rvert < V_{h_8}$	H4

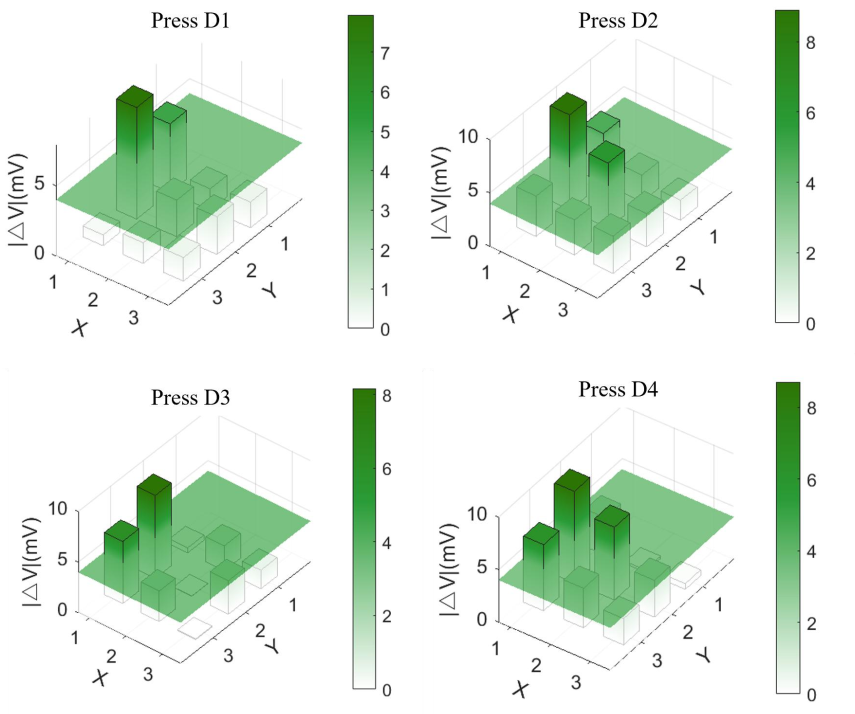

Supplementary Figure 12. Output comparison of pressing D1-D4.

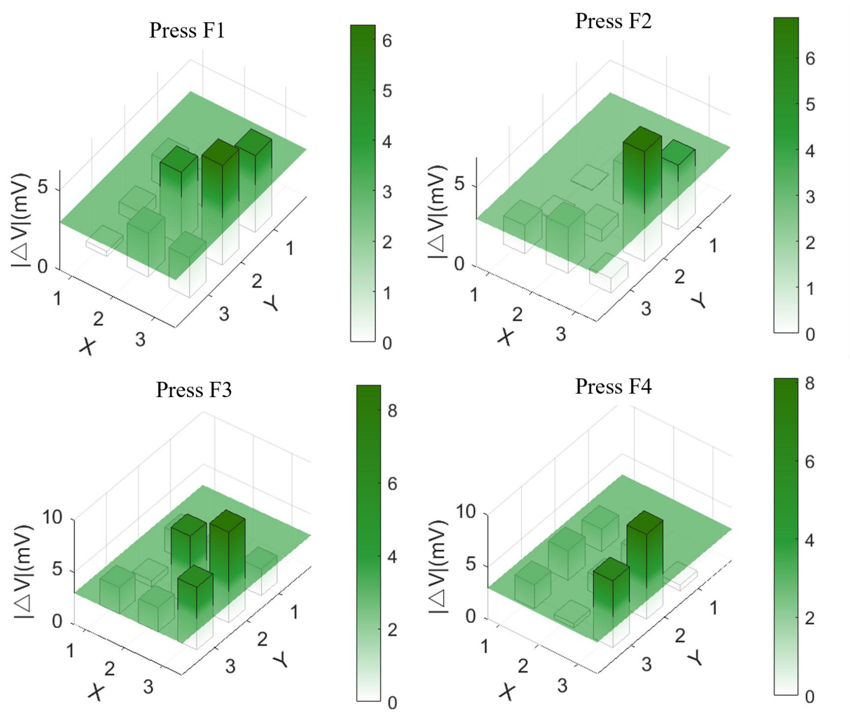

Supplementary Figure 13. Output comparison of pressing F1-F4.

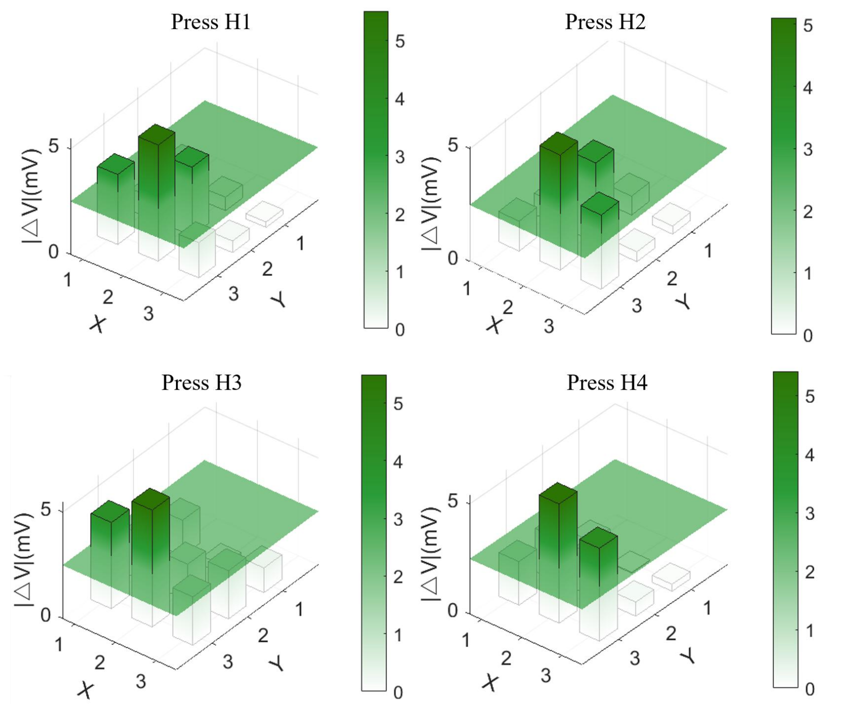

Supplementary Figure 14. Output comparison of pressing H1-H4.

Supplementary Table 7. Performance comparison of sensors with similar functions

Ref.	Magnetization method	Linearity*	Hall Sensor Types	Resolution
[4]	sinusoidal magnetization	N/A	Commercial: MLX90393	3*3
[5]	Symmetrical up and down	0.95	Commercial: MLX90393	2*2
[6]	Opposite magnetization	0.97	Commercial: MLX90393	4*4
Our work	Periodic magnetization	0.97	Graphene Hall sensor	6*6

Supplementary Material Appendix A

The Hall sensor detects this variation in the magnetic field and outputs a corresponding Hall voltage.

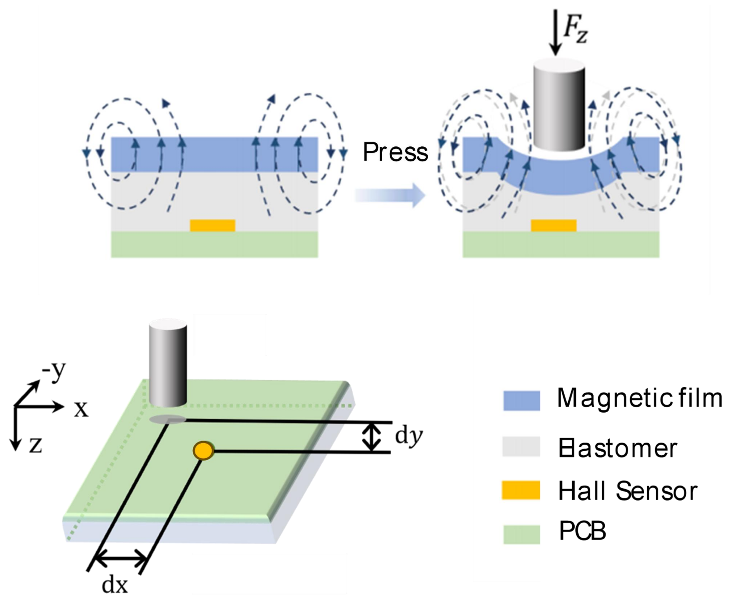

Figure A1-1. Schematic diagram of the magnetic tactile sensor.

For a magnetic film with a specific magnetization direction, when the film is not pressed, the initial magnetic field strength detected by the Hall sensor is:

$$B_{mag\_initial}=\frac{B_{disc}}{r_{disc}^3} \tag{A-1}$$

Where, B_{disc} is the initial magnetic field at the pressed point, and r_{disc} is the distance between the Hall sensor and the pressed point. This distance can also be expressed as:

$$r_{disc}=\sqrt{dx^2+dy^2+z_{disc}^2} \tag{A-2}$$

Here, dx is the x-component of the horizontal distance between the Hall sensor and the pressed point, dy is the y-component of the horizontal distance, and z_{disc} is the initial vertical distance between the Hall sensor and the pressed point. Substituting Equation (A-1) into Equation (A-2), we obtain:

$$B_{mag\_initial}=\frac{B_{disc}}{\left(dx^2+dy^2+z_{disc}^2\right)^{1.5}} \tag{A-3}$$

When a certain pressure F is applied to the magnetic film at the pressed point, the vertical displacement of the point is Δz. This results in a change in the magnetic flux density beneath the film. The variation in the magnetic field detected by the Hall sensor is expressed as:

$$\Delta B_{mag} \approx \left| \frac{\partial B_{mag}}{\partial z_{disc}} \right| \Delta z = \frac{3 B_{disc} z_{disc}}{\left(dx^2 + dy^2 + z_{disc}^2\right)^{2.5}} \Delta z \tag{A-4}$$

For a given force F applied by the 3D-printed cylindrical indenter, the indentation depth on the elastomer surface can be estimated as:

$$\Delta z = \frac{F(1-\upsilon^2)}{2 E r_a} \tag{A-5}$$

where υ is the Poisson's ratio of the material, E is the Young's modulus, and r_a is the radius of the cylindrical indenter. Substituting this expression into Equation (A-4), we obtain:

$$\Delta B_{mag} = \frac{3 z_{disc}(1-\upsilon^2)}{2 E r_a \left(dx^2 + dy^2 + z_{disc}^2\right)^{2.5}} B_{disc} F \tag{A-6}$$

It can be concluded that the magnetic field variation is approximately linearly proportional to the applied force. Defining the linear magnetoelastic coefficient as μ, we obtain $\Delta B_{mag} = \mu F$. Combining the Hall voltage formula, the relationship between the change in Hall voltage and the applied force can be derived as:

$$\Delta V_H = \frac{R_H}{H} I \Delta B_{mag} = \frac{R_H I}{H} \mu F \tag{A-7}$$

where H is the thickness of the Hall device, R_H is the Hall coefficient, and I is the magnitude of the current applied to the Hall element.